

FABRICATION OF TUNGSTEN NANOWIRES BY FOCUSED ION BEAM CHEMICAL VAPOUR DEPOSITION AND THEIR IN-SITU ELECTRICAL CHARACTERIZATION

SUDHANSHU SRIVASTAVA AND K. K. VERMA

Department of Physics and Electronics, Dr. R. M. L. Avadh University, Faizabad-224001 (U.P.), India

RECEIVED : 23 February, 2013

We report on the fabrication of W nanowires on SiO₂ substrate using focused ion beam induced deposition (FIB-CVD) and studies of I-V characteristics of the W nanowires have been investigated. The electrical resistivity of the material of FIB fabricated nanowires are found to be more than that of the bulk material. Also, the resistivity of W nanowires of fixed dimensions varies as a function of beam current used for their FIB deposition. An increment in the resistivity has been explained on the basis of high contamination of C, Ga etc. present in the FIB fabricated nanostructures.

INTRODUCTION

Nanostructure is gaining importance now-a-days due to its large surface area. The synthesis of nanostructure with controlled size and composition is of paramount importance. Since the physical gate length of transistor is ~20 nm and in view of the potentiality of device fabrication at molecular level, the importance of nanowire as interconnect has increased tremendously. Keeping in view of limitation of size of secondary cloud in several technique, FIB offers better option by limiting this secondary electrons clouds, thereby making precise milling. Due to this repairing of electronic device efficiently increases. FIB technology now has numerous important applications, such as Ga implantation and subsequent etching for the fabrication of electronic devices and circuits.

The physical and electrical properties drastically changes due to confinement effects and large surface area to volume ratio. The nanostructures of precise dimensions viz. nanopillars [1], wires, cantilevers, springs etc. are needed for the fabrication of nano/micro electromechanical systems (NEMS/MEMS) nanosensors and actuators [2] etc. The applications of the nanowires [4] are in nanoelectronics [5] particularly in making metallic contacts for single domain particles to investigate the fundamental optical, electrical, mechanical and magnetic properties. Keeping in view this fact the property of these nanowires itself need to be investigated. There are a variety of techniques for the fabrication of nanowires [6], such as thermal gas decomposition [7], laser ablation of powder targets [8] or hot filament chemical vapor deposition [9] etc. Most of them are based on the vapor-liquid-solid (vls) mechanism [10], in which various metals such as Au [6], Fe [10], Ti [11] or Ga [12] catalytically enhance the growth of nanowires. The liquid alloy cluster serves as a preferential site for adsorption of reactant from the vapour phase and when supersaturated act as the nucleation site for crystallization. The super saturation of the eutectic melt, which is established by catalytic absorption of gaseous reactants, acts as the driving force for growth in a highly anisotropic manner. In recent years, the focused ion beam (FIB) technology has been

recognized to have the ability to produce complex prototype 3D nano structures through a combination of gradual deposition and removal of material due to sputtering. The sputtering occurs when the incident ion beam transfers sufficient momentum to the surface and near surface atoms for them to escape through a cascade of collisions. For deposition, appropriate precursor gas is made available near the substrate through a gas nozzle whose molecules gets adsorbed and forms a monolayer on the surface. The deposition occurs due to layer by layer cracking of adsorbed precursor gas molecules into volatile and non volatile products under impact of energetic ions after which the nonvolatile components sticks to the surface while the volatile components escape. In this paper, the electrical transport properties of FIB fabricated W nanowires have been investigated.

EXPERIMENTAL WORK

The experiments were performed using a dual beam focused ion beam (FIB) system installed at IIT Kanpur. The system is equipped with field emission Ga ion source with energy range $\sim 10 - 30$ kV and beam current ~ 0.3 PA – 100 PA, high resolution (7 nm) ion optics, high resolution milling and gas chemistry functionalities for deposition of C, Pt and W along with e-beam patterning, scanning electron microscope (SEM) and energy dispersive spectroscopy (EDS) facilities. In the present experiments, Tungsten Hexa Carbonyl $W(CO)_6$ was used as a precursor gas for the deposition of W nanowires.

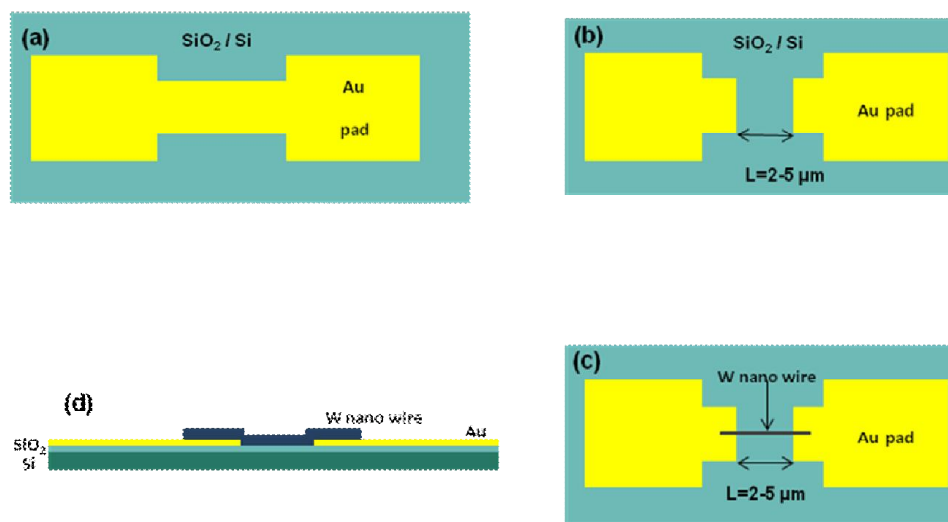


Figure 1: Strategy adopted to fabricate the electrical contacts. (a) A 500 nm thick SiO₂ layer grown on Si substrate by wet oxidation and then deposition of 100 nm gold using an I-shaped mask. (b) Isolation of gold macro contacts by ion milling. (c) Side view of W nanowires fabricated on SiO₂/Si wafer. (d) Top view of deposited W nanowires using FIB.

The strategy adopted for the fabrication of the electrical contacts for the characterization of W nanowires is shown in figure 1. A 500 nm thick SiO₂ layer grown on Si substrate by wet oxidation has been utilized as substrate for proper electrical insulation. An I-shaped mask having two square holes of dimension $1 \text{ mm} \times 1 \text{ mm}$ connected with a line of width $200 \mu\text{m}$ has been made. Gold film of thickness 100 nm has been thermally evaporated at a rate of $1 \text{ \AA}/\text{sec}$ on SiO₂/Si substrate through above pre-designed mask to obtain the structure as depicted in figure 1(a). The pressure inside the chamber was maintained at 2×10^{-6} mbar or

less during the evaporation. The gold deposited SiO_2 sample has been annealed in the atmosphere at temperature of 500°C for 30 minutes to improve the adhesion of the gold film.

The gold pads have been connected to the Keithley 6430 source meter and the sample has been mounted inside the FIB chamber.

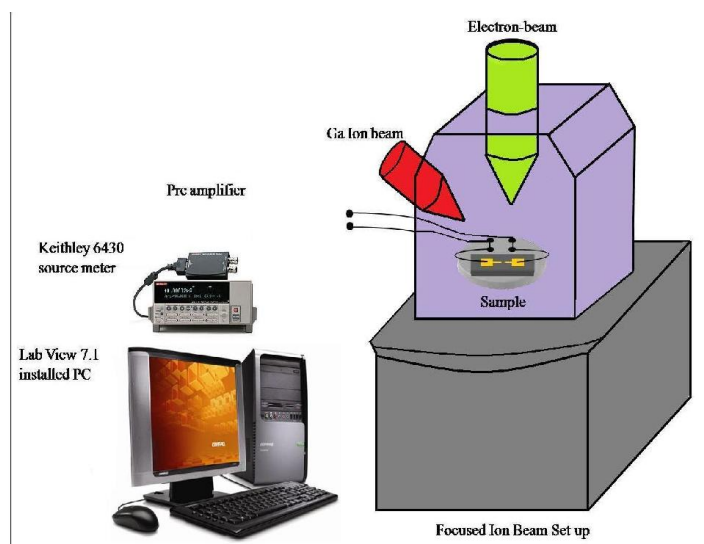


Figure 2. Schematic diagram of the experimental set up.

The whole experimental arrangement is shown in the figure 2. The gold line connecting the pads has been milled $3.64\ \mu\text{m}$ wide in the middle using FIB to isolate the macro pads as shown in figure 1 (b). We have fabricated several W nanowires having length of $3.64\ \mu\text{m}$ and width between $50\ \text{nm}$ to $300\ \text{nm}$. The I-V characteristics of these nanowires have been studied. Moreover, these W nanowires were analyzed energy dispersive spectroscopy and scanning electron microscopy.

RESULTS AND DISCUSSION

SEM image of a W nanowire of dimensions $50\ \text{nm} \times 3.64\ \mu\text{m} \times 200\ \text{nm}$ fabricated using $30\ \text{KeV}$ Ga FIB at a beam current of $100\ \text{pA}$ is shown in figure 3(a). Similar W nanowires with the width ranging from $50\ \text{nm}$ to $300\ \text{nm}$ have been fabricated and their I-V characteristics have been studied. The resistances of these nanowires have been calculated using the slope of the I-V curve. Figure 3 (b) shows the variation of resistance of the nanowires as a function of the wire width. From this plot we see that the resistivity starts to increase once the wire width decreases below $300\ \text{nm}$. This means there is a dependence of resistance on wire width. It has been observed that the resistance 'R' is inversely proportional to the nanowire width 'w'. The behaviour is similar as that of the bulk material. The resistivity of the W nanowires has been calculated which is found in the order of $10^{-3}\ \text{ohm-cm}$. The measured resistivity value is much larger than the bulk Tungsten resistivity $10^{-6}\ \text{ohms-cm}$. An increase in the resistivity value of the FIB fabricated nanostructures can be explained on the basis of contamination due to Ga, C etc. present in the structures as confirmed by the EDS analysis. The EDS spectrum depicts the presence of C and Ga in the W nanowires as shown in figure 4. Figure 3 (c) shows the variation of resistivity of the W nanowires as a function of the beam current which has been used for deposition of nanowires having cross sectional area 100

nm \times 250 nm and length 3.64 μ m. From this figure we can conclude that the resistivity of the nanowire starts to increase once the beam current decreases below 100 pA. This indicates the dependency of resistivity on beam current. The resistivity ' ρ ' decreases as a function of beam current used for deposition of nanowires. The reason behind this fact is an increment of the metallic content in the nanowire with an increase in the deposition current.

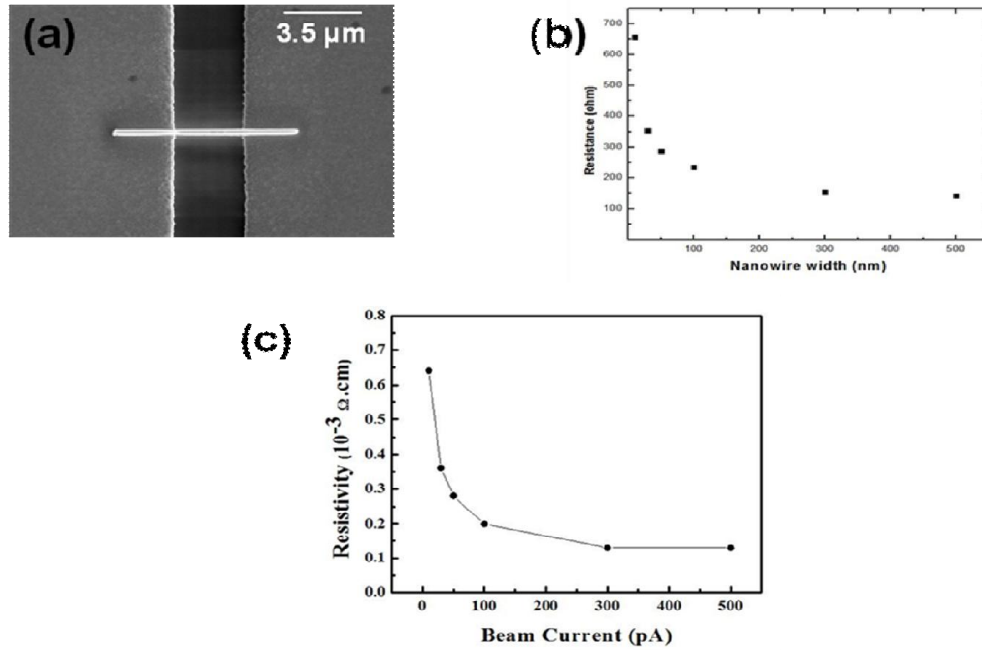


Figure 3: (a) SEM image of a W nanowire of dimensions 50 nm \times 3.64 μ m \times 200 nm fabricated using 30 KeV Ga FIB at a beam current of 100 pA. (b) Variation of resistance of the nanowires as a function of the wire width. (c) Variation of resistivity of the nanowires as a function of beam current.

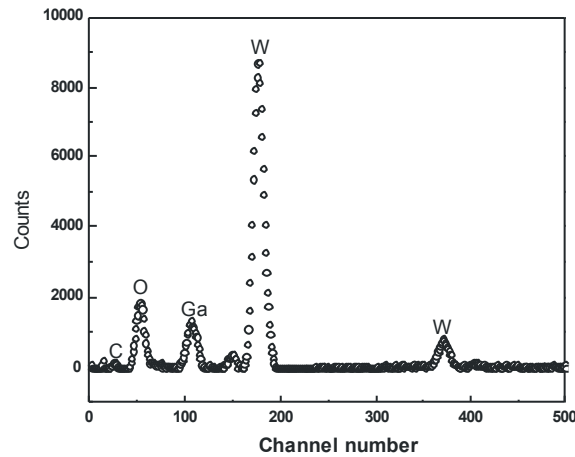


Figure 4: EDS spectrum taken on the W nanowire which depicts the presence of C and Ga

Table 1: represents the measured resistance of W nanowires having deposition current range from 10pA to 1000pA for 100nm wire. The values match well within the experimental error limit.

Table 1: Measured resistivity of W nanowires having current range from 10 pA to 500 pA.

Current for W dep (pA)	10	30	50	100	300	500
Resistivity single wire ($10^{-3} \Omega \text{ cm}$)	0.64	0.36	0.28	0.20	0.13	0.13

CONCLUSION

W nanowires have been fabricated on SiO_2 substrate using focused ion beam and the electrical transport properties studies have been carried out. The resistivity of the material of FIB fabricated nanowires are found more than that of the bulk material which may be due to the contamination of carbon, gallium etc. present in the FIB fabricated nanostructures. Also, it has been observed that higher beam current results into a low resistivity wire.

ACKNOWLEDGEMENTS

We thank the staff of the Ion Beam Laboratory at IIT Kanpur for their assistance. We are thankful to late V.N. Kulkarni, Indian Institute of Technology, Kanpur for providing the FIB system for our study.

REFERENCES

1. Ishida, M., Fujita, J., Ichihashi, T., Ochiai, Y., Kaite, T., MatSui, S., *J. Vac. Sci. Technol.*, **B21(6)**, 2728 – 2731 Nov/Dec (2003).
2. Tripathi, S. K., Shukla, N., Dhamodaran, S. and Kulkarni, V. N., *Nanotechnology*, **19**, 205302 (2008).
3. Hu, J. T., Odom, T. W. and Lieber, C. M., *Acc. Chem. Res.*, **32**, 435 (1999).
4. Lugsten, A, Bernardi, J., Tomastik, C., Bertagnolli, E., *Appl. Phys. Lett.*, **88**, 163114 (2006).
5. Orlov, A.O., Amlani, I., Bernstein, G.H., Lent, C.S. and Snider, G.L., *Science*, **277**, 928 (1997).
6. Health, J. R. and Legous, F.K., *Chem. Phys. Lett.*, **208**, 263 (1993).
7. Morales, A.M. and Leiber, C.M., *Science*, **279**, 208 (1998).
8. Zhou, X. T., Wang, N., Lai, H. L., Peng, H. Y., Bello, I., Wongand, N. B., Lee, O. S., *Appl. Phys. Lett.*, **74**, 3942 (1999).
9. Wagner, R. S. and Ellis, W.C., *Appl. Phys. Lett.*, **4**, 89 (1964).
10. Pearson, A.L., Larson, M. L., Stenstrim, S., Ohlsson, B. J., Samuelson, L. and Wallenberg, L. R., *Nature*, **3**, 677 (2004).
11. Kamins, T. I., Williams, R. S., Cheng, Y., Chang, Y. L. and Chang, Y. A., *Appl. Phys. Lett.*, **76**, 562 (2000).
12. Sukasha, M. K., Sharma, S., Miranda, R., Lian, G. and Dicky, E. C., *Appl. Phys. Lett.*, **79**, 1546 (2001).
13. Jiantao, H., Teri, W. O. and Leiber, C. M., *Acc. Chem. Res.*, **32**, 435 (1999).

□